© 2021. Published by The Company of Biologists Ltd | Development (2021) 148, dev199717. doi:10.1242/dev.199717

REVIEW

From whole organism to ultrastructure: progress in axonal imaging for decoding circuit development

Cory J. Weaver and Fabienne E. Poulain*

ABSTRACT

Since the pioneering work of Ramón y Cajal, scientists have sought to unravel the complexities of axon development underlying neural circuit formation. Micrometer-scale axonal growth cones navigate to targets that are often centimeters away. To reach their targets, growth cones react to dynamic environmental cues that change in the order of seconds to days. Proper axon growth and guidance are essential to circuit formation, and progress in imaging has been integral to studying these processes. In particular, advances in high- and super-resolution microscopy provide the spatial and temporal resolution required for studying developing axons. In this Review, we describe how improved microscopy has revolutionized our understanding of axonal development. We discuss how novel technologies, specifically light-sheet and super-resolution microscopy, led to new discoveries at the cellular scale by imaging axon outgrowth and circuit wiring with extreme precision. We next examine how advanced microscopy broadened our understanding of the subcellular dynamics driving axon growth and guidance. We finally assess the current challenges that the field of axonal biology still faces for imaging axons, and examine how future technology could meet these needs.

KEY WORDS: Axon guidance, Growth cone, Connectomes, Brain wiring, Super-resolution

Introduction

How our brain develops and operates has captivated the mind of scientists for centuries. Our knowledge in neuroscience was notably revolutionized at the dawn of the 20th century when Ramón y Cajal settled a long-standing debate regarding the fundamental architecture of the nervous system. Using a staining method developed by his ideological opponent, Camillo Golgi, Ramón y Cajal showed neurons to be discrete cells rather than a continuous, interconnected network (Ramón y Cajal, 1991; Sotelo, 2002). This theory, the neuron doctrine, became a fundamental principle of neuroscience and prompted the advent of studies aimed at understanding how neurons form complex, yet precise, neural circuits. During development, neurons extend highly dynamic axons that interpret guidance cues in their environment to navigate towards their final synaptic targets. This pathfinding is ensured by motile structures at axonal ends, the growth cones, that respond to the numerous extracellular signals they encounter via receptors present on their surface. Axons often extend great distances from the soma and adopt distinct behaviors to ensure the accuracy of circuit wiring. Axons not only grow, pause and turn, but also fasciculate (bundle) with each other, repel one another and retract or degenerate after taking erroneous paths (Poulain and Chien, 2013; Spead and Poulain, 2020; Tessier-Lavigne and Goodman, 1996; Wang and Marquardt, 2013). Early light microscopy and electron microscopy (EM) studies have highlighted the morphological features of individual neurons and their axonal projections in various tissues. In contrast, recent advances in imaging technologies, including light-sheet fluorescent microscopy (LSFM) and super-resolution microscopy (SRM), have provided insights into axonal development in unparalleled detail, enabling the reconstruction of neural circuits *in vivo* and the discovery of the cellular and molecular mechanisms governing circuit development (Maglione and Sigrist, 2013). In this Review, we highlight major advances in the field of axon development driven by technological progress in microscopy. We first present major contributions and limitations of EM and conventional light microscopy to our understanding of developing axons. We then introduce recent findings in axon growth, guidance and circuit wiring achieved via LSFM and SRM. We highlight how these new technologies have provided an improved, integrated view of circuits and developmental processes *in vivo*. We further describe breakthroughs in defining molecular signaling pathways that govern axon growth and guidance, focusing on signal integration at the axonal membrane and cytoskeletal dynamics. We finally explore how emerging technologies can push the boundaries of axonal imaging to further decode the intricate mechanisms of circuit development *in vivo*.

Imaging axons and circuits: from past to present

Since Ramón y Cajal's seminal work on brain architecture, developmental neurobiologists have taken advantage of constantly improving labeling and imaging techniques to dissect the morphology of neurons and the cellular organization of complex circuits across species. Axonal projections were first visualized by light microscopy in fixed tissues after filling neurons with a dye, allowing the reconstruction of neuronal tracts and patterns of connectivity from serial sections. This technique was notably used in the 1960s and 1970s to trace axons in various ganglia of small invertebrate models (Davis, 1970; Kerkut et al., 1970; Stretton and Kravitz, 1968). Serial electron micrographs also largely contributed to these early mapping efforts, leading to the reconstruction of the entire nervous system in *C. elegans* and *Drosophila* (White et al., 1986; Zheng et al., 2018), and the first characterization of fine intra-axonal components such as neurofilaments and microtubules (Wuerker and Kirkpatrick, 1972). Later on, the introduction of improved anterograde and retrograde tracers combined with fluorescent immunolabeling broadened the characterization of anatomical circuits by enabling the simultaneous visualization of multiple axonal tracts together with identified neurons (Gerfen and Sawchenko, 1985; van der Kooy and Steinbusch, 1980). Coupled with the development of high-resolution confocal laser scanning microscopy in the 1990s, these tracing and labeling approaches were

Department of Biological Sciences, University of South Carolina, Columbia, SC 29208, USA.

*Author for correspondence (fpoulain@mailbox.sc.edu)

C.J.W., 0000-0003-2203-9881; F.E.P., 0000-0002-7867-748X

Development (2021) 148, dev199717. doi:10.1242/dev.199717

instrumental for delineating axonal projections in vertebrates at different stages of development and their organization into topographic maps in sensory systems (Harris, 1986; McLaughlin and O'Leary, 2005). Axons were also found to adapt to the environment they navigate in, correcting their trajectories after embryological manipulations (Guthrie and Lumsden, 1992). Concomitant progress in genetics with the advent of gene targeting and genetic screens enabled the identification of signaling factors required for proper axon guidance and circuit formation. Ephrins, for example, were discovered as the main guidance cues governing the targeting of retinal axons in the optic tectum (Frisen et al., 1998; Nakamoto et al., 1996).

Neuro-anatomical tracing and EM drove our current understanding of axonal development and circuit wiring but nonetheless present shortcomings, the most notable being their incompatibility with live imaging. In addition, some axonal structures do not survive the fixation process during EM and are therefore difficult to identify from a micrograph (Leterrier et al., 2017; Letourneau, 2009). The discovery of fluorescent proteins together with the development of molecular and viral tools to label specific cells, structures or proteins addressed these challenges and opened a new era in the study of developing axons. It became possible not only to visualize axon and growth cone dynamics within an organism (Higashijima et al., 2000; Knobel et al., 1999; Murray et al., 1998; Zallen et al., 1999), but also to monitor and track intra-axonal processes sustaining axonal behavior. Anterograde transport of cytoskeletal proteins, for example, was known to exist from pulse-chase radiolabeling experiments conducted in the 1970s (Hoffman and Lasek, 1975; Willard et al., 1979) but only became fully appreciated after neurofilaments tagged with green fluorescent protein (GFP) were observed to have rapid anterograde movements separated by long pauses in live cultured neurons (Roy et al., 2000; Wang et al., 2000). This 'Stop and Go' model of slow axonal transport was also found to apply to microtubules (Wang and Brown, 2002). GFP and cytoskeletal regulators fused to fluorescent proteins were also expressed in developing neurons in *C. elegans* and visualized by *in vivo* time-lapse confocal imaging, leading to the identification of essential signaling pathways regulating growth cone organization and protrusive activity during axon formation and guidance (Adler et al., 2006; Chang et al., 2006; Quinn et al., 2008; Norris et al., 2009). Finally, the use of fluorescent proteins enabled the visualization and functional characterization of receptors at the surface of growth cones and axons (O'Donnell et al., 2009). For example, fusions of the receptor Robo to GFP or its pH-sensitive variant pHLuorin have been used to monitor the targeting and trafficking of Robo at the surface of navigating axons *in vivo*, leading to the discovery of molecular mechanisms fine-tuning the responsiveness of axons to the guidance cue Slit (Keleman et al., 2005; Pignata et al., 2019). Altogether, decades of research in developmental neurobiology has exploited the major advances in tracing, genetic engineering and imaging mentioned above to paint the detailed picture of axonal development and circuit wiring we have today. We have characterized the outgrowth and trajectories of many axonal tracts during development in various species, identified most guidance factors instructing how circuits are built, and deciphered many intra-cellular cascades underlying growth cone responses to guidance cues (Dudanova and Klein, 2013; Gorla and Bashaw, 2020; McCormick and Gupton, 2020; Spead and Poulain, 2020; Stoeckli, 2018; Suárez et al., 2014). Yet many questions remain unanswered due to limitations in imaging techniques. Although confocal microscopy has clear advantages for live-imaging axons, it is restrained by a diffraction limit of ∼200 nm (Maglione and Sigrist, 2013), which prevents the resolution of individual axons in a densely packed nerve bundle, let alone axonal structures separated by only a few tens of nanometers. We are thus still limited in our understanding of how individual axons elongate, communicate with one another or change their behavior to form an entire nervous system. Similarly, although we have identified cues, receptors and intra-axonal processes regulating axon guidance, we do not know how these factors and structures operate and are spatially and temporally regulated at the molecular scale. Progress in these areas require imaging modalities capable of nanometer-scale resolution, large fields of view and live analysis that we are only beginning to achieve and have only recently led to major breakthroughs.

Capturing axon growth and guidance in developing neural circuits

Deciphering how individual axons develop into precise neuronal networks *in vivo* requires improved spatial and temporal resolution to observe fine structural details and fast dynamic processes, all the while limiting photobleaching and phototoxicity for live imaging. Recent advances in genetic, imaging and computational processing have addressed these challenges and opened a new era in the study of circuit wiring by enabling the visualization of single axons *in vivo* and the reconstruction of entire connectomes.

Detailing single axons in complex circuits across species

A major advance in our understanding of circuit wiring came with the development of genetic approaches that specifically label multiple individual axons within a brain structure, thereby providing a unique way to map neuronal connectivity over long distances with remarkable resolution. Among them, Brainbow and its derivatives proved to be especially powerful as they use a recombinase-mediated DNA inversion or excision strategy to stochastically express a unique combination of green, red and blue fluorescent proteins within a cell (Cai et al., 2013; Lichtman et al., 2008; Livet et al., 2007; Weissman and Pan, 2015). As the combination of these three primary colors generates all colors in the visual spectrum, each Brainbow-expressing neuron displays a unique, distinct color that allows visualization and tracing of its axonal projection. Combined with confocal microscopy, the Brainbow approach was first used to visualize individual oculomotor and hippocampal mossy fiber axons in the adult brain, and to reconstruct 341 mossy fiber axons and 93 of their postsynaptic targets, the granule cells, in the cerebellum (Livet et al., 2007). Multicolor tracing with Brainbow has since been adapted to multiple organisms and used in various systems to delineate the precise architecture of circuits and identify underlying wiring mechanisms (Egawa et al., 2013; Hadjieconomou et al., 2011; Hampel et al., 2011; Heap et al., 2013; Pan et al., 2011; Robles et al., 2013). The recent reconstruction of 71 retinal ganglion cell (RGC) projections in the dorsal lateral geniculate nucleus, for example, led to the discovery that multiple retinal axons converge onto relay cells in that region, challenging the textbook notion that each relay cell receives input from only one or two RGCs in the adult (Hammer et al., 2015).

Concomitant with the development of Brainbow and other labeling approaches, progress in microscopy has tremendously increased both the acquisition speed and three-dimensional resolution of imaging, thereby allowing the reconstruction of axonal projections in exquisite detail (Table 1). LSFM notably differs from confocal microscopy in that it illuminates a sample with a thin sheet of light perpendicular to the axis of fluorescence

Development (2021) 148, dev199717. doi:10.1242/dev.199717

Table 1. Comparison of technical approaches for axonal imaging

Imaging technique	Lateral resolution	Axial resolution	Advantages	Disadvantages
EM	<1 nm	40 nm	High lateral and axial resolution	Only applicable to fixed tissues Limited sub-cellular labeling Cytoskeletal structures hard to preserve Expertise required for specimen preparation, expensive equipment required
Wide-field microscopy	200-300 nm	500-700 nm	Low photobleaching and phototoxicity High acquisition speed Uses standard dyes and fluorophores Low cost, easy to use	Low lateral and axial resolution High non-specific background No optical sectioning possible
Confocal microscopy	150-250 nm	500-600 nm	Non-invasive optical sectioning Live 3D multi-color imaging Uses standard dyes and fluorophores	Diffraction-limited resolution Slow to moderate acquisition speed High photobleaching and phototoxicity
LSFM	150-200 nm	200-300 nm	Live 3D multi-color imaging of large specimen Low photobleaching and phototoxicity High acquisition speed Long-term imaging Uses standard dyes and fluorophores	Diffraction-limited resolution
SRM: SIM	100 nm	200-300 nm	Moderate lateral resolution Live 3D multi-color imaging Relatively large fields of view Uses standard dyes and fluorophores	Slow acquisition speed Super-resolution achieved through image processing: possible artifacts Limited axial resolution Sensitive to out-of-focus light (high labeling density signals are harder to image)
SRM: STED	30-50 nm	100-200 nm	High lateral resolution Fast acquisition speed with parallelized scanning Live 3D multi-color imaging Uses standard dyes and fluorophores No data processing required	High photobleaching and phototoxicity High labeling density required
SRM: PALM/STORM	10-40 nm	10-50 nm	High lateral and axial resolution Live 3D multi-color imaging Low photobleaching and phototoxicity	Limited to thin specimens Slow acquisition speed Uses non-standard dyes or fluorescent proteins Complex data processing, possible artifacts

EM, electron microscopy; LSFM, light-sheet fluorescent microscopy; PALM, photo-activated localization microscopy; SIM, structural illumination microscopy; SRM, super-resolution microscopy; STED, stimulated emission depletion; STORM, stochastic optical reconstruction microscopy.

detection (Voie et al., 1993). The coincidence of the light sheet with the focal plane of the fluorescence detection system restricts the excitation of fluorophores to the illuminated plane, thereby avoiding phototoxicity or photobleaching and enabling fast imaging of large biological specimens from multiple different directions over long periods of time (Huisken et al., 2004; Keller and Stelzer, 2008; Tomer et al., 2012). Axial resolution and sensitivity of LSFM are determined by the thickness of the light sheet, which varies depending on how the sheet is generated. For example, sub-diffraction limit resolution has been achieved using ultrathin optical lattices to image both non-neuronal cells (Chen et al., 2014; Gao et al., 2012; Wan et al., 2019) and neurons (Corsetti et al., 2019; Lemon and Keller, 2015; Liu et al., 2018). Different methods can be used to create light sheets, and we refer interested readers to excellent recent reviews for more technical details (Albert-Smet et al., 2019; Hillman et al., 2019; Wan et al., 2019). Thanks to its advantages, LSFM has rapidly been employed in combination with solvent-clearing methods for imaging neural circuits in whole embryos with unprecedented resolution (Mano et al., 2018; Ueda et al., 2020). Opaque embryos rendered transparent with solvent-based clearing procedures such as 3DISCO [three-dimensional imaging of solvent cleared organs (Ertürk et al., 2012)] or its more-recent derivatives iDISCO or uDISCO (Pan et al., 2016; Renier et al., 2014) can be immunostained and imaged, allowing the precise tracing of axonal projections together with their molecular identification. When used on mouse transgenic embryos, this approach has led to the three-dimensional reconstruction of motor and sensory projections with unparalleled precision, enabling the visualization of fine motor axon terminal arborizations from individual forelimb nerves (Belle et al., 2014; Liau et al., 2018). More recently, 36 cleared human embryos and fetuses ranging from 6 to 14 weeks of gestation were immunostained with over 70 antibodies and imaged with LSFM to generate the most advanced three-dimensional atlas of human development at the cellular resolution (Belle et al., 2017). The entire human peripheral nervous system was reconstructed over time, providing a precise developmental time-lapse of the sensory innervation of the human hand (Fig. 1). Interestingly, a striking variability in the innervation of the left and right hands was observed, with the left and right ulnar and radial nerves harboring noticeable differences in branch number and length (Belle et al., 2017). Heterogeneity in wiring was similarly observed in *Drosophila* using LSFM combined with

Development (2021) 148, dev199717. doi:10.1242/dev.199717

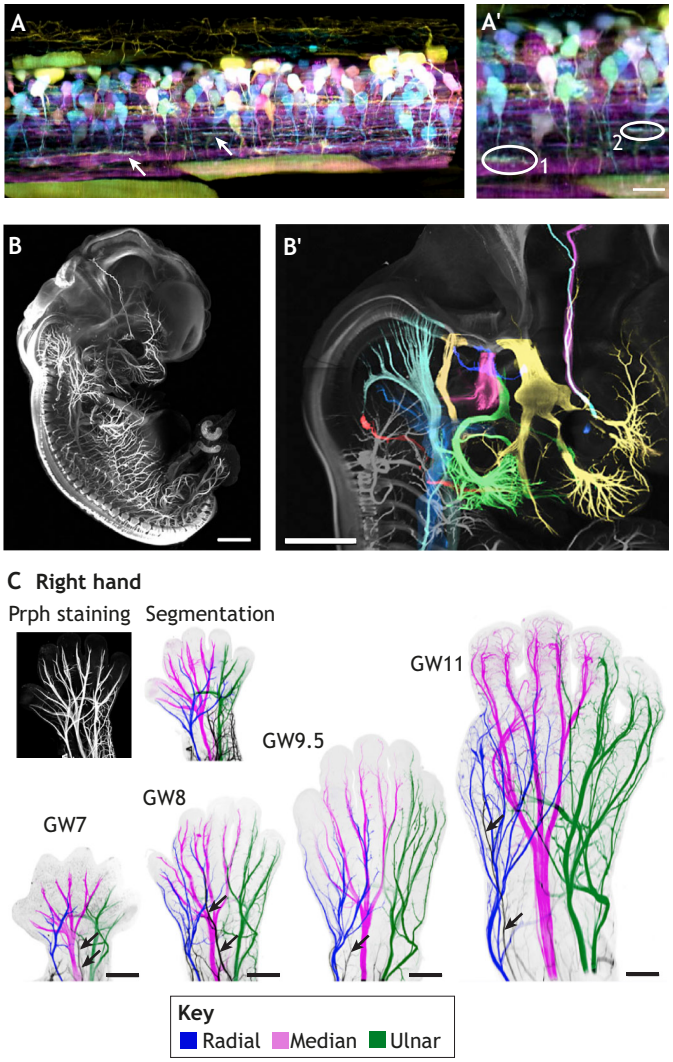

Fig. 1. LSFM offers an unparalleled view of neural circuits in whole embryos. (A) *In vivo* imaging of developing neurons in the zebrafish spinal cord at 58 hours post-fertilization. Newly differentiated neurons express a stochastic combination of three fluorophores, allowing the visualization and tracing of their axons and growth cones (arrows). (A′) Zoomed view of growth cones from rostrocaudally projecting axons. Scale bar: 10 µm. Adapted, with permission, from Liu et al. (2018). 1 and 2, regions in A indicated by arrows. (B) Visualization of the peripheral nervous system in a human embryo at gestation week 7 (GW7). Peripheral nerves were immunostained using antibodies against the intermediate filament protein peripherin (Prph). Scale bar: 1 mm. (B′) Right view of the head and cranial nerves at GW7. Cranial nerves were segmented and highlighted with specific pseudo-colors. Cyan, vagus and trochlear; blue, spinal accessory; green, facial; yellow, trigeminal; light pink, oculomotor; dark pink, vestibulocochlear; red, hypoglossus; dark blue, Haller's anastomosis. Scale bar: 1 mm. Adapted, with permission, from Belle et al. (2017).
(C) Innervation of the developing human right hand from GW7 to GW11. Individual sensory nerves stained for Prph were segmented and color-coded in blue (radial nerves), green (ulnar nerves) and magenta (median nerves). Black arrows indicate the musculocutaneous nerve extending into the hand. Scale bars: 400 µm; 700 µm (top left inset). Adapted, with permission, from Belle et al. (2017).

expansion microscopy, a method whereby a biological sample is physically enlarged using an isotopically expanding polymer (Gao et al., 2019). Long-range tracing of olfactory projection neurons elongating from the antenna lobe to the calyx of the mushroom body and lateral horn revealed subcellular wiring details that varied among samples analyzed. The size and number of boutons formed in the calyx notably differed among neurons from a same hemisphere as well as between animals (Gao et al., 2019). Thus, by enabling the visualization and three-dimensional reconstruction of axonal trajectories *in vivo* at high resolution, LSFM has brought to light previously uncharacterized anatomical details of circuits and their variability across individuals.

Monitoring axonal behavior in developing embryos

Although reconstructing precise connectomes from cleared samples provides invaluable insight into the developmental trajectories that axons take to form circuits (Friedmann et al., 2020), it does not provide a dynamic view of how these axons elongate and find their way to their final target. A major advance in that field came with the use of LSFM on transparent model organisms such as *C. elegans* or zebrafish (Abu-Siniyeh and Al-Zyoud, 2020; van Krugten et al., 2021). Thanks to the increased imaging speed and low phototoxicity provided by LSFM, transgenic embryos can now be continuously imaged during embryogenesis, providing an unprecedented ability to monitor axonal behaviors and growth cone dynamics over long periods of time *in vivo*. Changes in growth cone morphology were correlated with guidance decisions made by neurites circumnavigating the nerve ring in *C. elegans* after imaging embryos every 2 s for 14 h (Wu et al., 2011). Computational tracking of the movements made by ALA mechanosensory neurons and their neurites in elongating embryos further revealed that anterior-posterior neurite outgrowth starts towards the end of elongation and continues after cells reach their final positions (Christensen et al., 2015). In zebrafish, live LSFM was used to visualize branchiomotoneuron axon outgrowth and sensory cranial ganglion projections (Ingold et al., 2015; Zecca et al., 2015). *In vivo* time-lapse analysis of sensory neurons notably revealed a link between neuronal differentiation and the topography of sensory projections: the site of differentiation prefigures the location where sensory axons enter the hindbrain, whereas the order of differentiation determines the mediolateral topography of the sensory bundles within the hindbrain (Zecca et al., 2015). More recently, imaging of axons and growth cones in the spinal cord of zebrafish embryos in which a subset of newly differentiated neurons were genetically labeled with fluorophores led to the discovery of different modes of elongation: growth cones of axons migrating in the rostrocaudal direction explore their environment in the direction of their motion, whereas growth cones of dorsoventrally aligned axons probe across a larger two-dimensional fan (Liu et al., 2018) (Fig. 1). LSFM has also been coupled with lineage-tracing algorithms and functional ablation approaches to delineate principles of network assembly in *C. elegans* and discover an essential role for pioneer neurons in strata formation (Moyle et al., 2021).

Discovering novel phenotypes in signaling mutants

Along with establishing how the birth, position or migration of neurons influences the spatiotemporal dynamics of axon growth and circuit wiring, LSFM has allowed the discovery of subtle phenotypes in signaling mutants that would have been challenging to reveal with earlier methods. For example, live imaging of cranial motor axon outgrowth in zebrafish embryos uncovered a novel function for the cell-adhesion molecule MDGA2A. In absence of MDGA2A, branchiomotor axons make pathfinding mistakes and exhibit increased collateral branching and defasciculation (axons aberrantly leave from axonal bundles) (Ingold et al., 2015). In the mouse, three-dimensional imaging of immunolabeled axonal tracts in

Development (2021) 148, dev199717. doi:10.1242/dev.199717

Box 1. Brief overview of the different types of SRM

Structural illumination microscopy (SIM)
The sample is illuminated with periodic excitation patterns (structured illumination) of high spatial frequency in different orientations (Gustafsson, 2000). A super-resolution image is obtained by calculating the interference (moiré) patterns obtained from multiple images. SIM can be used on samples prepared for standard fluorescence microscopy and can achieve lateral and axial resolutions of about 100 nm and 200 nm, respectively.

Stimulated emission depletion microscopy (STED)
The excitation beam of the microscope is overlaid with a doughnut-shaped, red-shifted depletion beam to quench the fluorescence emitted at the periphery of the diffraction-limited excitation spot, thereby restricting fluorescence emission to the center of the doughnut (Hell and Wichmann, 1994). STED achieves high spatial and temporal resolutions (60 nm and below), but its application for large-volume imaging is limited.

Stochastic optical reconstruction microscopy (STORM) and photo-activated localization microscopy (PALM)
A small subset of fluorescent molecules is repeatedly photo-activated with a light at low intensity, imaged and photo-bleached. The low number of activated molecules enables the recording of their position at each iteration of photo-switching. A super-resolution image is reconstructed by superimposing multiple wide-field images containing the localized single-molecule positions (Shcherbakova et al., 2014). PALM and STORM can achieve a localization precision of 10 nm, allowing the study of protein distribution at the molecular level. However, they necessitate the use of photo-activatable fluorescent proteins (PALM) or photo-switching pairs of cyanine dyes (STORM) (Lakadamyali et al., 2012).

Point accumulation for imaging in nanoscale topography (PAINT)
Being conceptually similar to STORM, PAINT relies on the transient binding of diffusing fluorescent probes to the structure of interest. Fluorescent probes are not visible due to their rapid motion, but become visible as they are immobilized upon binding. Probes can then be imaged until they are bleached or become mobile again (Sharonov and Hochstrasser, 2006).

netrin 1 (*Ntn1*), *Dcc* and *Robo3* mutants unraveled specific and unexpected defects in medial habenula axons forming the fasciculus retroflexus (FR) tract (a tract that relays information from the habenula to the interpeduncular nucleus of the limbic midbrain) (Belle et al., 2014). FR axons surprisingly cross the floor plate but then turn back and coalesce at the midline in *Robo3* mutants, which differs from the guidance errors made by other commissural tracts. Conversely, FR axons not only fail to cross the midline but also show additional fasciculation and pathfinding defects in *Ntn1* and *Dcc* mutants, demonstrating distinct, specific functions for these guidance signaling pathways in the habenular system (Belle et al., 2014). As the fine details of circuit wiring can now be resolved, researchers have begun to revisit the role of well-known signaling pathways in brain development. For example, LSFM was recently combined with a novel eye-clearing method to reassess the role of DCC in the visual system (Vigouroux et al., 2020). Retinal axons were found to stall at the optic disk and make pathfinding errors in central visual centers that persist postnatally in the absence of DCC in the retina (Vigouroux et al., 2020). Altogether, by allowing imaging of the nervous system like never before, LSFM offers a detailed and dynamic picture of circuit wiring *in vivo* that not only extends our understanding of how the brain forms in four dimensions, but also shines new light on the molecular mechanisms governing nervous system assembly. The parallel development of SRM has further revolutionized the study of axons at the mesoscale range, casting a spotlight on how intra-axonal structures and protein dynamics underlie the adaptive response of axons to their environment.

Zooming in on the molecular mechanisms driving axon growth and guidance

Deciphering how individual axons assemble into circuits requires the ability to resolve sub-axonal structures and signaling complexes at the nanoscale resolution. The recent advent of SRM (see Box 1 for a brief overview of SRM techniques, including SIM and PAINT) has transformed our view of the molecular processes driving axon growth and guidance by enabling the visualization of cell-surface receptors, organelles, actin and microtubule cytoskeletons, and intracellular signaling events below the diffraction limit, in the 10-100 nm range (Fig. 2). SRM has notably enhanced the axial resolution of imaging from about 500 nm (resolution of confocal miscroscopy) to 50-200 nm (see Table 1 for details) (Gustafsson et al., 2008; Hein et al., 2008; Jones et al., 2011), thereby allowing unprecedented observations in three dimensions.

Visualizing receptor trafficking and signaling dynamics

Axons respond to a panoply of attractive and repulsive factors present in their environment to find their way to their post-synaptic target. Their responsiveness to these guidance cues is dictated by the presence of corresponding receptors at the growth cone surface and varies spatially and temporally depending on receptor availability. The distribution of receptors is indeed dynamic, with receptors actively targeted to the plasma membrane by exocytosis, redistributed across the membrane by lateral diffusion, or removed from the plasma membrane by endocytosis or extracellular cleavage (Zang et al., 2021). Although confocal imaging has been instrumental in defining the repertoire of receptors expressed by a given axon at a specific time, the diffraction-limited resolution it achieves does not allow for the characterization of receptors and their dynamics at the molecular level. We do not know, for example, how many receptors must interact with each other to transduce signals or whether they need to be targeted to specialized sub-domains at the plasma membrane to do so. In contrast to confocal microscopy, SRM offers a unique opportunity to address these questions by enabling the precise visualization of single molecular complexes in living cells at the nanoscale resolution. Dual-color stochastic optical reconstruction microscopy (STORM) imaging of the membrane protein caveolin 3 and the ryanodine receptor RyR in cardiac myocytes, for example, reveals distinct localizations for both proteins, demonstrating that their apparent colocalization observed by confocal microscopy is actually caused by optical blurring (Baddeley et al., 2011) (Fig. 2A,A′).

Elegant studies have first employed SRM to dissect the nanoscale organization of receptors at the synapse. Glutamate AMPA receptors, for example, were found to concentrate in sub-synaptic domains of about 70 nm and randomly diffuse between them within seconds by lateral diffusion (Nair et al., 2013). Similarly, metabotropic glutamate receptors mGluR4s and the adhesion molecule neurexin 1 appear organized in small, discrete nanodomains at pre-synaptic active zones (Siddig et al., 2020; Trotter et al., 2019). A similar partitioned organization of receptors and adhesion molecules has more recently been observed along the axon shaft. STORM and stimulated emission depletion (STED) imaging studies have revealed that the endocannabinoid receptor CB1 and the neural cell-adhesion molecule NCAM1 are both distributed into clusters that are evenly spaced along axons, with a periodicity of about 190 nm (Li et al., 2020; Zhou et al., 2019). Interestingly, this distribution coincides with the membrane-

Development (2021) 148, dev199717. doi:10.1242/dev.199717

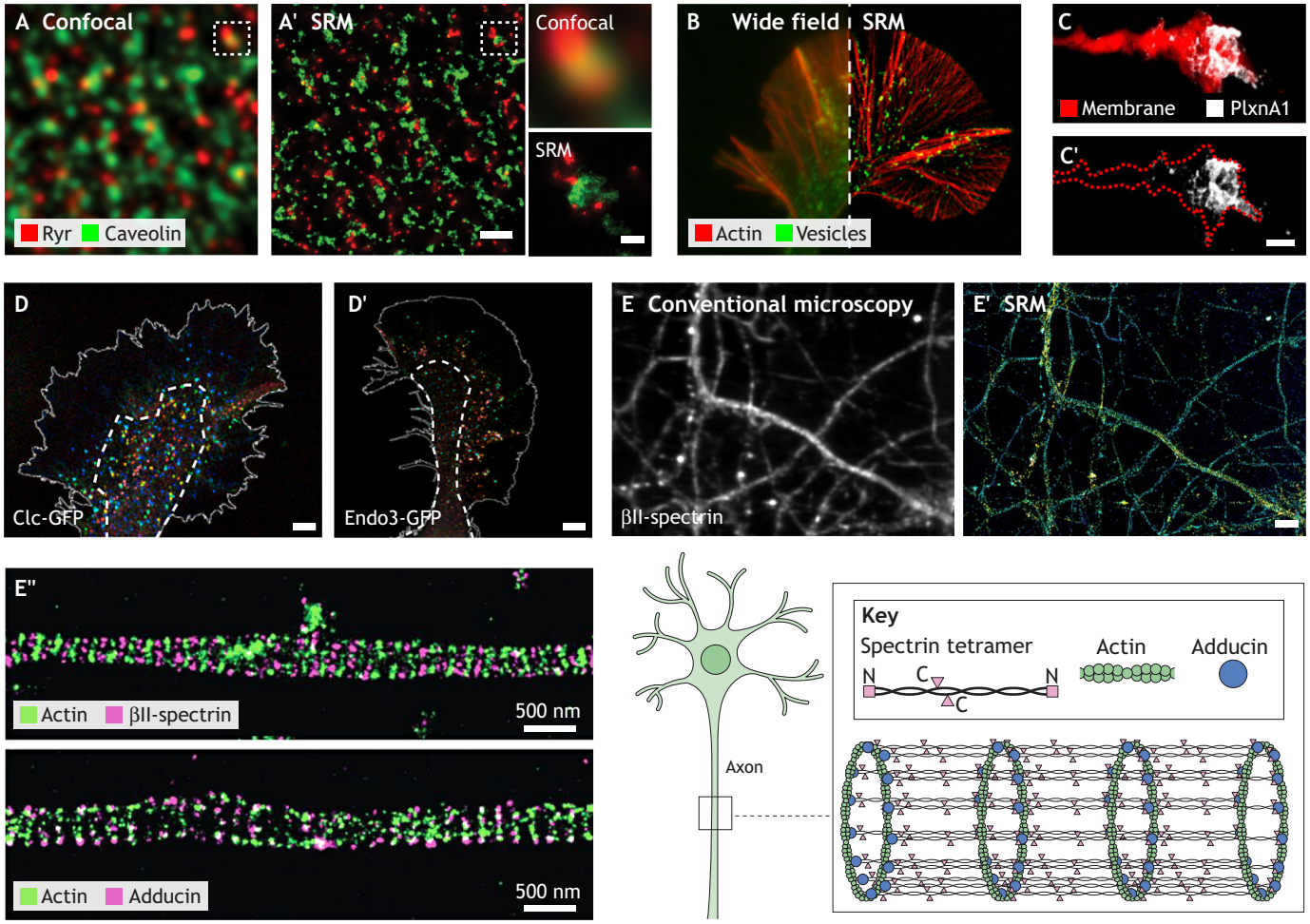

Fig. 2. SRM reveals intra-axonal structures and signaling complexes with nanoscale resolution. (A,A′) When compared with confocal microscopy, super-resolution microscopy (SRM) resolves the distribution of multiple proteins at and near the plasma membrane. Distribution of ryanodine receptors (red) and caveolin (green) in isolated rat cardiac myocytes visualized by confocal microscopy (A) or SRM (STORM) (A′). Scale bars: 1 µm; 200 nm (zoom panels). Adapted from Baddeley et al. (2011), where it was published under a CC-BY 4.0 license. (B) SRM reveals cytoskeletal and transport dynamics. Actin filaments (red) and vesicles (green) of a growth cone visualized by wide-field imaging or SRM (SIM). Adapted, with permission, from Nozumi et al., 2017. (C,C′) SRM reveals receptor trafficking at the growth cone. Live STED imaging of the plexin A1 receptor fused to pHLuorin at the plasma membrane (red) of a commissural growth cone (dotted line) entering the midline (open book preparation). Scale bar: 2 µm. Adapted, with permission, from Pignata et al. (2019). (D,D′) SRM reveals different types of endocytosis. Pseudo-colored SIM images of fixed growth cones expressing clathrin light chain or endophilin 3 fused to GFP (Clc-GFP in D, Endo3-GFP in D′). Clathrin-mediated endocytosis mostly occurs in the central domain of the growth cone, whereas endophilin-mediated endocytosis occurs at the leading edge. Scale bars: 2 µm. Adapted, with permission, from Nozumi et al. (2017). (E-E″) SRM reveals the periodic organization of actin rings in the axon shaft. Distribution of βII-spectrin in cultured neurons visualized by conventional microscopy (E) or SRM (E′). (E″) Two-color STORM imaging reveals that actin, βII-spectrin and adducin form ring-like structures wrapping around the circumference of the axon (see diagram). Scale bars: 2 µm in E,E′, 500 nm in E″. Adapted, with permission, from Xu et al. (2013).

associated periodic skeleton (MPS): actin, spectrin and associated molecules generate a braided lattice along axons, with actin forming ring-like structures wrapping around the axonal circumference that are evenly spaced every ∼180 to 190 nm (Vassilopoulos et al., 2019; Xu et al., 2013) (Fig. 2E-E″). The MPS acts as a signaling platform that CB1 and NCAM1 are recruited to upon activation by agonists, leading to the trans-activation of receptor tyrosine kinases and associated downstream signaling (Zhou et al., 2019). As both NCAM1 and CB1 are known to regulate axon guidance and fasciculation (Berghuis et al., 2007; Hansen et al., 2008; Mulder et al., 2008; Saez et al., 2020), it will be interesting to test how their trafficking and compartmentalized signaling contributes to the formation of neural circuits.

Changes in the nanoscale distribution of receptors play a major role in regulating the responsiveness of elongating axons to extracellular factors. A remarkable study illustrated this notion perfectly by tracking the distribution of plexin and Robo receptors at the surface of spinal commissural axons crossing the midline at the floor plate (Pignata et al., 2019). Midline crossing requires axons to change their sensitivity to the floor plate-derived repulsive cues Slit and semaphorin 3B (Zou et al., 2000). Initially insensitive, axons become responsive as they reach the midline, thereby being propelled away from that region as they cross it. STED analysis of axons in spinal cord open book preparations revealed that commissural growth cones alter the presentation of plexin A1 (Plxna1) and Robo1 receptors in a specific spatio-temporal sequence as they approach the midline (Pignata et al., 2019). Plxna1 is delivered to the growth cone surface during navigation through the first half of the floor plate (from the floor plate entry to the midline), whereas Robo1 appears at the plasma membrane only when growth cones navigate through the second half. Interestingly, Plxna1 predominantly accumulates at the front of the growth cone (Fig. 2C,C′), whereas

Development (2021) 148, dev199717. doi:10.1242/dev.199717

Robo1 concentrates at its rear. The recruitment of receptors to the plasma membrane correlates with changes in growth cone behavior: growth cones slow down after gaining Plxna1 but increase their exploratory behavior along the rostro-caudal axis as Robo1 appears at the surface. Whereas Plxna1 maintains its restricted localization during growth cone pathfinding to the midline, the distribution of Robo1 actively changes and becomes more diffuse as the growth cone reaches the floor plate exit (Pignata et al., 2019). Altogether, these detailed observations underscore that receptors are extremely dynamic and must be delivered to the surface of growth cones at specific times and locations for proper axon navigation and circuit wiring.

Membrane dynamics not only ensure proper trafficking of receptors to and from the plasma membrane but also mediate the response of a growth cone to a cue. Seminal studies using total internal reflection fluorescence microscopy (TIRFM) coupled with calcium uncaging revealed that an imbalance between exocytosis and endocytosis downstream of calcium signaling is required for steering the growth cone in one direction (Tojima et al., 2014). VAMP2-mediated exocytosis exceeds clathrin-mediated endocytosis to ensure proper growth cone turning towards a factor. Conversely, predominant endocytosis mediates repulsion (Tojima et al., 2014). Interestingly, endocytosis at the leading edge of the growth cone was recently found to be clathrin independent (Nozumi et al., 2017). Instead, analysis of vesicular trafficking in growth cones by structural illumination microscopy (SIM) has identified a novel type of endocytosis at the leading edge that relies on endophilin and is linked to F-actin bundling (Fig. 2D,D′). Endophilin-mediated endocytosis removes cholesterol-rich membrane domains such as lipid rafts and appears to sustain growth cone morphology and axon outgrowth (Nozumi et al., 2017). The importance of vesicular release for proper axonal navigation has conversely recently been demonstrated *in vivo*. Using deconvolution coupled with stepwise optical saturation microscopy (DeSOS) on confocal time-lapse images to achieve super-resolution (Zhang et al., 2019), researchers detected an accumulation of synaptic vesicles in pioneer growth cones of dorsal root ganglia sensory axons as axons crossed the dorsal root entry zone (DREZ) in zebrafish (Nichols and Smith, 2019a). Interestingly, the matrix metalloproteinase MMP14a was found to colocalize with growth cone actin clusters at the DREZ. Preventing vesicular release or inhibiting MMP14a disturbed pioneer axon spinal invasion, suggesting that the delivery of synaptic-like vesicles and MMP14a at the DREZ decision point enables growth cone navigation across the glial limitans. Importantly, vesicular accumulation was found to depend on the formation of actin-based invasive protrusions, demonstrating an essential role for cytoskeletal rearrangements in axon pathfinding (Nichols and Smith, 2019a).

Focusing on cytoskeletal dynamics driving axon growth and pathfinding

The actin cytoskeleton has long been known to be crucial for proper axon pathfinding (Gomez and Letourneau, 2014). Filamentous actin (F-actin) accumulates at the growth cone and actively polymerizes, depolymerizes and assembles into a mesh or bundles to form peripheral lamellipodia or filopodia, respectively. Actin polymerization and recycling are especially important for growth cone adaptive responses as they provide the forces driving filopodial and lamellipodial explorative protrusions. Recent studies have taken advantage of SRM to discover novel mechanisms regulating actin dynamics in growth cones. For example, tracking of single molecules using photo-activated localization microscopy (PALM) coupled to TIRFM revealed that the core planar cell polarity protein Vangl2 reduces axon elongation by decreasing the mechanical coupling between N-cadherin adhesions and the retrograde actin flow (Dos-Santos Carvalho et al., 2020). F-actin was also found by STED microscopy to depend on the centrosome and the translocation of somatic F-actin from the cell body, as its treadmilling speed significantly decreases after centrosomal disruption (Meka et al., 2019). SRM has further led to the discovery of additional F-actin structures sustaining growth cone behaviors. F-actin-rich puncta were detected by SIM in the central region of growth cones where they colocalize with point-contact and invadosomal proteins such as integrin and cortactin (Santiago-Medina et al., 2015). The resulting apical invadosomal protrusions were shown to dynamically extend from the central domain and to contain proteases such as ADAM17. Inhibiting invadosome formation strongly decreases the extension of motor axons into the peripheral myotome in *Xenopus*, suggesting that invadosomal proteolytic activity might be required for local extracellular matrix degradation and growth cone advance (Santiago-Medina et al., 2015). Similarly in zebrafish, invadosomes were observed to form in the central domain of pioneer sensory growth cones as they enter the DREZ, and blocking their formation prevents sensory axons from entering the spinal cord (Nichols and Smith, 2019b). Altogether, these studies highlight an important and conserved function of invadosomes in axon navigation *in vivo*.

Besides new actin arrangements in growth cones, SRM has revealed unanticipated actin structures along axons. For example, observation of actin dynamics using DeSOS super-resolution time-lapse imaging in zebrafish revealed the existence of actin accumulations at the basis of extending neurites named stable base clusters. These clusters form and disappear immediately before the initiation and retraction of neurites, suggesting that their presence dictates neurite formation (Zhang et al., 2019). Along the axon shaft, SRM has revealed the organization of the MPS and its regulation by non-muscle myosin II to ensure axon radial contractility (Costa et al., 2020; Vassilopoulos et al., 2019; Wang et al., 2020; Xu et al., 2013). SRM has also led to the refined characterization of axonal actin waves and trails. Actin waves were initially characterized as growth cone-like membrane protrusions forming at the base of neurites and migrating to their ends at an average speed of ∼2-3 µm min^{-1} (Ruthel and Banker, 1998). Because of their anterograde transport and eventual fusion with growth cones, actin waves have been proposed to support fast axonal elongation (Flynn et al., 2009; Ruthel and Banker, 1998). However, a recent study using live STED imaging challenged this hypothesis by observing a decrease in neurite elongation speed (to about 0.5 µm min^{-1}) in the presence of actin waves (Mortal et al., 2017). Actin waves appeared to play a role in maintaining growth cone motility rather than controlling neurite elongation. They were also found to have a different nanoscale organization of acto-myosin structures that sustain a distinct mode of movement compared with growth cones (Mortal et al., 2017). In addition to actin waves, focal hotspots of actin spaced at ∼3-4 µm along axons have recently been detected by live STORM imaging (Ganguly et al., 2015). These hotspots were found to serve as actin polymerization sites that generate long filaments named actin trails that extend bidirectionally along the axon shaft. Although their function still remains unknown, actin trails have been proposed to participate in the slow transport of actin in axons and mediate actin enrichment at pre-synaptic boutons.

F-actin works in concert with microtubules to modulate growth cone advance and steering. In fact, both microtubule transport and

Development (2021) 148, dev199717. doi:10.1242/dev.199717

polymerization play a major role in axon elongation and guidance (Poulain and Sobel, 2010). Yet the respective contribution of microtubule assembly versus transport to axon elongation has remained a controversial debate for decades. Recent SRM studies have provided new insight by visualizing the dynamics of individual microtubules during axon growth. Single-molecule switching nanoscopy conducted on *Aplysia californica* growth cones revealed that inhibiting microtubule assembly decreases both microtubule extension in the growth cone and the association between the motor protein dynein and microtubules, indicating that microtubule dynamics are actually required for dynein-mediated microtubule translocation (McElmurry et al., 2020). Additional STED and SIM studies have shown that microtubule dynamics are controlled by actin itself in the growth cone. In *Xenopus*, microtubules and F-actin were found to align in the growth cone periphery to mediate proper growth cone response to guidance cues (Slater et al., 2019). In contrast, growth cones were found to contain myosin II-generated actin arcs that prevent microtubules from extending in the growth cone, thereby promoting axon pausing (Schaefer et al., 2002; Dupraz et al., 2019). The Rho-GTPase RhoA regulates the formation of these actin arcs, thereby controlling the duration of growth and pause phases that dictate the speed of axon elongation (Dupraz et al., 2019). Interestingly, a recent study challenged the importance of actin arcs for regulating axon growth *in vivo* (Santos et al., 2020). Whereas actin arcs are observed in growth cones extending in two-dimensional substrates, they are lacking in growth cones navigating in three-dimensional collagen or hyaluronic acid matrices. Consequently, unrestrained microtubules extend into the leading edge of growth cones, thereby promoting faster axonal elongation (Santos et al., 2020). Altogether, these results indicate a different mode of axon growth in a three-dimensional environment and highlight the importance of using SRM on more physiological models to define the molecular mechanisms sustaining axon elongation *in vivo*.

Conclusions and perspectives

The advent of LSFM and SRM has propelled the study of neuronal circuit wiring into a new era by offering an unprecedented view of the structural and molecular components governing axon development and network assembly. Yet deciphering precisely how a multitude of axons elongating at the same time *in vivo* interpret their environment in a specific manner to find their post-synaptic targets remains a challenging task. Axons often behave differently *in vitro* versus *in vivo* and can navigate over long distances in deep locations that are difficult to image at high resolution. Our ability to 'see individual trees in detail, while still looking over the whole forest', as Maglione and Sigrist elegantly said (Maglione and Sigrist, 2013), will require imaging modalities that combine large-volume and deep-tissue imaging with nanoscale resolution and fast acquisition.

High acquisition speed is crucial for visualizing developing axons in a constantly changing environment *in vivo*. LSFM has achieved millisecond-scale imaging of neuronal activity in zebrafish brains (Farrar et al., 2018; Haslehurst et al., 2018), but it lacks nanoscale spatial resolution. Current studies are addressing acquisition speed by reducing the number of exposures needed for STORM imaging (Gaire et al., 2021) or by combining LSFM with a radial fluctuation Bayesian analysis (Chen et al., 2020). Used to image the intact brain in *Drosophila*, the latter approach was able to resolve individual axon terminals with a spatial resolution of 70 nm and at speeds that were two orders of magnitude faster than previous single-molecule techniques (Chen et al., 2020). On the other end of the spectrum, SRM has facilitated the detection of molecular complexes at a mesoscale resolution but has mostly been used on cultured cells or fixed tissue sections to overcome the limited penetration of fluorescent signals in live tissue. To circumvent that problem, several groups are now combining STED with two-photon excitation in order to reveal structural details and conduct live-cell imaging in deep brain tissue (Bethge et al., 2013; Ding et al., 2009; Nägerl et al., 2008). Although no single technology has yet been developed to image large volumes in deep tissues at high speed and super-resolution, single molecule-guided Bayesian localization microscopy (SIMBA) and its derivatives offer some promise (Xu et al., 2017). Indeed, SIMBA provides exceptional spatial (50 nm) and temporal (0.15 to 0.2 s) resolutions, and does not require specialized SRM setups necessary for STED, SIM or PALM/STORM, making it more accessible. Notably, open-source plug-ins that run on simple desktop machines are available for SIMBA processing (Li et al., 2020). Last but not least, recent technological developments are poised to transform our analysis of axon behavior by allowing the observation of molecular interactions at high resolution *in vivo*. For example, two-color STED has just recently been combined with Förster resonance energy transfer (FRET) to image protein-protein interactions at a single-molecule detection level (Szalai et al., 2021). The prospect of combining SRM with optogenetic control of axon guidance (Endo et al., 2016; Harris et al., 2020) for directly manipulating axons and developing circuits *in vivo* also promises an exciting future in developmental neurosciences.

Acknowledgements

The authors apologize for omitting any references owing to space restrictions and thank all reviewers for their constructive feedback.

Competing interests

The authors declare no competing or financial interests.

Funding

This research was supported by the National Institutes of Health/ National Institute of Neurological Disorders and Stroke (R01NS109197 to F.E.P.) and an Aspire I grant from the Office of the Vice President for Research at the University of South Carolina (to C.J.W). Deposited in PMC for release after 12 months.

References

Abu-Siniyeh, A. and Al-Zyoud, W. (2020). Highlights on selected microscopy techniques to study zebrafish developmental biology. *Lab. Anim. Res.* **36**, 12. doi:10.1186/s42826-020-00044-2

Adler, C. E., Fetter, R. D. and Bargmann, C. I. (2006). UNC-6/Netrin induces neuronal asymmetry and defines the site of axon formation. *Nat. Neurosci.* **9**, 511-518. doi:10.1038/nn1666

Albert-Smet, I., Marcos-Vidal, A., Vaquero, J., Desco, M., Muñoz-Barrutia, A. and Ripoll, J. (2019). Applications of light-sheet microscopy in microdevices. *Front. Neuroanat* **13**, 1. doi:10.3389/fnana.2019.00001

Baddeley, D., Crossman, D., Rossberger, S., Cheyne, J., Montgomery, J., Jayasinghe, I., Cremer, C., Cannell, M. and Soeller, C. (2011). 4D super-resolution microscopy with conventional fluorophores and single wavelength excitation in optically thick cells and tissues. *PLoS ONE* **6**, e20645. doi:10.1371/journal.pone.0020645

Belle, M., Godefroy, D., Dominici, C., Heitz-Marchaland, C., Zelina, P., Hellal, F., Bradke, F. and Chédotal, A. (2014). A simple method for 3D analysis of immunolabeled axonal tracts in a transparent nervous system. *Cell Rep.* **9**, 1191-1201. doi:10.1016/j.celrep.2014.10.037

Belle, M., Godefroy, D., Couly, G., Malone, S., Collier, F., Giacobini, P. and Chédotal, A. (2017). Tridimensional visualization and analysis of early human development. *Cell* **169**, 161-173.e12. doi:10.1016/j.cell.2017.03.008

Berghuis, P., Rajnicek, A., Morozov, Y., Ross, R., Mulder, J., Urbán, G., Monory, K., Marsicano, G., Matteoli, M., Canty, A. et al. (2007). Hardwiring the brain: endocannabinoids shape neuronal connectivity. *Science* **316**, 1212-1216. doi:10.1126/science.1137406

Bethge, P., Chéreau, R., Avignone, E., Marsicano, G. and Nägerl, U. (2013). Two-photon excitation STED microscopy in two colors in acute brain slices. *Biophys. J.* **104**, 778-785. doi:10.1016/j.bpj.2012.12.054

Cai, D., Cohen, K., Luo, T., Lichtman, J. and Sanes, J. (2013). Improved tools for the Brainbow toolbox. *Nat. Methods* **10**, 540-547. doi:10.1038/nmeth.2450
Chang, C., Adler, C. E., Krause, M., Clark, S. G., Gertler, F. B., Tessier-Lavigne, M. and Bargmann, C. I. (2006). MIG-10/lamellipodin and AGE-1/PI3K promote axon guidance and outgrowth in response to slit and netrin. *Curr. Biol.* **16**, 854-862. doi:10.1016/j.cub.2006.03.083
Chen, B., Legant, W., Wang, K., Shao, L., Milkie, D., Davidson, M., Janetopoulos, C., Wu, X., Hammer, J., Liu, Z. et al. (2014). Lattice light-sheet microscopy: imaging molecules to embryos at high spatiotemporal resolution. *Science* **346**, 1257998. doi:10.1126/science.1257998
Chen, R., Zhao, Y., Mengna, L., Wang, Y., Zhang, L. and Fei, P. (2020). Efficient super-resolution volumetric imaging by radial fluctuation Bayesian analysis light-sheet microscopy. *J. Biophotonics* **13**, e201960242.
Christensen, R., Bokinsky, A., Santella, A., Wu, Y., Marquina-Solis, J., Guo, M., Kovacevic, I., Kumar, A., Winter, P., Tashakkori, N. et al. (2015). Untwisting the Caenorhabditis elegans embryo. *eLife* **4**, e10070. doi:10.7554/eLife.10070.058
Corsetti, S., Gunn-Moore, F. and Dholakia, K. (2019). Light sheet fluorescence microscopy for neuroscience. *J. Neurosci. Methods* **319**, 16-27. doi:10.1016/j.jneumeth.2018.07.011
Costa, A., Sousa, S., Pinto-Costa, R., Mateus, J., Lopes, C., Costa, A., Rosa, D., Machado, D., Pajuelo, L., Wang, X. et al. (2020). The membrane periodic skeleton is an actomyosin network that regulates axonal diameter and conduction. *Elife* **9**, e55471. doi:10.7554/eLife.55471.sa2
Davis, W. (1970). Motoneuron morphology and synaptic contacts: determination by intracellular dye injection. *Science* **168**, 1358-1360. doi:10.1126/science.168.3937.1358
Ding, J., Takasaki, K. and Sabatini, B. (2009). Supraresolution imaging in brain slices using stimulated-emission depletion two-photon laser scanning microscopy. *Neuron* **63**, 429-437. doi:10.1016/j.neuron.2009.07.011
Dos-Santos Carvalho, S., Moreau, M., Hien, Y., Garcia, M., Aubailly, N., Henderson, D., Studer, V., Sans, N., Thoumine, O. and Montcouquiol, M. (2020). Vangl2 acts at the interface between actin and N-cadherin to modulate mammalian neuronal outgrowth. *eLife* **9**, e51822. doi:10.7554/eLife.51822
Dudanova, I. and Klein, R. (2013). Integration of guidance cues: parallel signaling and crosstalk. *Trends Neurosci.* **36**, 295-304. doi:10.1016/j.tins.2013.01.007
Dupraz, S., Hilton, B., Husch, A., Santos, T., Coles, C., Stern, S., Brakebusch, C. and Bradke, F. (2019). RhoA controls axon extension independent of specification in the developing brain. *Curr. Biol.* **29**, 3874-3886.e9. doi:10.1016/j.cub.2019.09.040
Egawa, R., Hososhima, S., Hou, X., Katow, H., Ishizuka, T., Nakamura, H. and Yawo, H. (2013). Optogenetic probing and manipulation of the calyx-type presynaptic terminal in the embryonic chick ciliary ganglion. *PLoS ONE* **8**, e59179. doi:10.1371/journal.pone.0059179
Endo, M., Hattori, M., Toriyabe, H., Ohno, H., Kamiguchi, H., Iino, Y. and Ozawa, T. (2016). Optogenetic activation of axon guidance receptors controls direction of neurite outgrowth. *Sci. Rep.* **6**, 23976. doi:10.1038/srep23976
Ertürk, A., Becker, K., Jährling, N., Mauch, C., Hojer, C., Egen, J., Hellal, F., Bradke, F., Sheng, M. and Dodt, H. (2012). Three-dimensional imaging of solvent-cleared organs using 3DISCO. *Nat. Protoc.* **7**, 1983-1995. doi:10.1038/nprot.2012.119
Farrar, M., Kolkman, K. and Fetcho, J. (2018). Features of the structure, development, and activity of the zebrafish noradrenergic system explored in new CRISPR transgenic lines. *J. Comp. Neurol.* **526**, 2493-2508. doi:10.1002/cne.24508
Flynn, K., Pak, C., Shaw, A., Bradke, F. and Bamburg, J. (2009). Growth cone-like waves transport actin and promote axonogenesis and neurite branching. *Dev. Neurobiol.* **69**, 761-779. doi:10.1002/dneu.20734
Friedmann, D., Pun, A., Adams, E., Lui, J., Kebschull, J., Grutzner, S., Castagnola, C., Tessier-Lavigne, M. and Luo, L. (2020). Mapping mesoscale axonal projections in the mouse brain using a 3D convolutional network. *Proc. Natl. Acad. Sci. USA* **117**, 11068-11075. doi:10.1073/pnas.1918465117
Frisen, J., Yates, P. A., McLaughlin, T., Friedman, G. C., O'Leary, D. D. and Barbacid, M. (1998). Ephrin-A5 (AL-1/RAGS) is essential for proper retinal axon guidance and topographic mapping in the mammalian visual system. *Neuron* **20**, 235-243. doi:10.1016/S0896-6273(00)80452-3
Gaire, S., Wang, Y., Zhang, H., Liang, D. and Ying, L. (2021). Accelerating 3D single-molecule localization microscopy using blind sparse inpainting. *J. Biomed. Opt.* **26**, 026501. doi:10.1117/1.JBO.26.2.026501
Ganguly, A., Tang, Y., Wang, L., Ladt, K., Loi, J., Dargent, B., Leterrier, C. and Roy, S. (2015). A dynamic formin-dependent deep F-actin network in axons. *J. Cell Biol.* **210**, 401-417. doi:10.1083/jcb.201506110
Gao, R., Asano, S., Upadhyayula, S., Pisarev, I., Milkie, D., Liu, T., Singh, V., Graves, A., Huynh, G., Zhao, Y. et al. (2019). Cortical column and whole-brain imaging with molecular contrast and nanoscale resolution. *Science* **363**, eaau8302. doi:10.1126/science.aau8302
Gao, L., Shao, L., Higgins, C., Poulton, J., Peifer, M., Davidson, M., Wu, X., Goldstein, B. and Betzig, E. (2012). Noninvasive imaging beyond the diffraction limit of 3D dynamics in thickly fluorescent specimens. *Cell* **151**, 1370-1385. doi:10.1016/j.cell.2012.10.008
Gerfen, C. and Sawchenko, P. (1985). A method for anterograde axonal tracing of chemically specified circuits in the central nervous system: combined Phaseolus vulgaris-leucoagglutinin (PHA-L) tract tracing and immunohistochemistry. *Brain Res.* **343**, 144-150. doi:10.1016/0006-8993(85)91168-0
Gomez, T. and Letourneau, P. (2014). Actin dynamics in growth cone motility and navigation. *J. Neurochem.* **129**, 221-234. doi:10.1111/jnc.12506
Gorla, M. and Bashaw, G. (2020). Molecular mechanisms regulating axon responsiveness at the midline. *Dev. Biol.* **466**, 12-21. doi:10.1016/j.ydbio.2020.08.006
Gustafsson, M. (2000). Surpassing the lateral resolution limit by a factor of two using structured illumination microscopy. *J. Microsc.* **198**, 82-87. doi:10.1046/j.1365-2818.2000.00710.x
Gustafsson, M. G. L., Shao, L., Carlton, P. M., Wang, C. J. R., Golubovskaya, I. N., Cande, W. Z., Agard, D. A. and Sedat, J. W. (2008). Three-dimensional resolution doubling in wide-field fluorescence microscopy by structured illumination. *Biophys. J.* **12**, 4957-4970. doi:10.1529/biophysj.107.120345
Guthrie, S. and Lumsden, A. (1992). Motor neuron pathfinding following rhombomere reversals in the chick embryo hindbrain. *Development* **114**, 663-673. doi:10.1242/dev.114.3.663
Hadjieconomou, D., Rotkopf, S., Alexandre, C., Bell, D., Dickson, B. and Salecker, I. (2011). Flybow: genetic multicolor cell labeling for neural circuit analysis in Drosophila melanogaster. *Nat. Methods* **8**, 260-266. doi:10.1038/nmeth.1567
Hammer, S., Monavarfeshani, A., Lemon, T., Su, J. and Fox, M. (2015). Multiple retinal axons converge onto relay cells in the adult mouse thalamus. *Cell Rep* **12**, 1575-1583. doi:10.1016/j.celrep.2015.08.003
Hampel, S., Chung, P., McKellar, C., Hall, D., Looger, L. and Simpson, J. (2011). Drosophila Brainbow: a recombinase-based fluorescence labeling technique to subdivide neural expression patterns. *Nat. Methods* **8**, 253-259. doi:10.1038/nmeth.1566
Hansen, S., Berezin, V. and Bock, E. (2008). Signaling mechanisms of neurite outgrowth induced by the cell adhesion molecules NCAM and N-cadherin. *Cell. Mol. Life Sci.* **65**, 3809-3821. doi:10.1007/s00018-008-8290-0
Harris, W. (1986). Homing behaviour of axons in the embryonic vertebrate brain. *Nature* **320**, 266-269. doi:10.1038/320266a0
Harris, J., Wang, A., Boulanger-Weill, J., Santoriello, C., Foianini, S., Lichtman, J., Zon, L. and Arlotta, P. (2020). Long-range optogenetic control of axon guidance overcomes developmental boundaries and defects. *Dev. Cell* **53**, 577-588.e7. doi:10.1016/j.devcel.2020.05.009
Haslehurst, P., Yang, Z., Dholakia, K. and Emptage, N. (2018). Fast volume-scanning light sheet microscopy reveals transient neuronal events. *Biomed. Opt. Express* **9**, 2154-2167. doi:10.1364/BOE.9.002154
Heap, L., Goh, C., Kassahn, K. and Scott, E. (2013). Cerebellar output in zebrafish: an analysis of spatial patterns and topography in eurydendroid cell projections. *Front. Neural Circuits* **7**, 53. doi:10.3389/fncir.2013.00053
Hein, B., Willig, K. I. and Hell, S. W. (2008). Stimulated emission depletion (STED) nanoscopy of a fluorescent protein-labeled organelle inside a living cell. *Proc. Natl. Acad. Sci. USA* **105**, 14271-14276. doi:10.1073/pnas.0807705105
Hell, S. and Wichmann, J. (1994). Breaking the diffraction resolution limit by stimulated emission: stimulated-emission-depletion fluorescence microscopy. *Opt. Lett.* **19**, 780-782. doi:10.1364/OL.19.000780
Higashijima, S., Hotta, Y. and Okamoto, H. (2000). Visualization of cranial motor neurons in live transgenic zebrafish expressing green fluorescent protein under the control of the islet-1 promoter/enhancer. *J. Neurosci.* **20**, 206-218. doi:10.1523/JNEUROSCI.20-01-00206.2000
Hillman, E., Voleti, V., Li, W. and Yu, H. (2019). Light-Sheet Microscopy in Neuroscience. *Annu. Rev. Neurosci.* **42**, 295-313. doi:10.1146/annurev-neuro-070918-050357
Hoffman, P. and Lasek, R. (1975). The slow component of axonal transport. Identification of major structural polypeptides of the axon and their generality among mammalian neurons. *J. Cell Biol.* **66**, 351-366. doi:10.1083/jcb.66.2.351
Huisken, J., Swoger, J., Del Bene, F., Wittbrodt, J. and Stelzer, E. (2004). Optical sectioning deep inside live embryos by selective plane illumination microscopy. *Science* **305**, 1007-1009. doi:10.1126/science.1100035
Ingold, E., Vom Berg-Maurer, C., Burckhardt, C., Lehnherr, A., Rieder, P., Keller, P., Stelzer, E., Greber, U., Neuhauss, S. and Gesemann, M. (2015). Proper migration and axon outgrowth of zebrafish cranial motoneuron subpopulations require the cell adhesion molecule MDGA2A. *Biol. Open* **4**, 146-154. doi:10.1242/bio.20148482
Jones, S. A., Shim, S. H., He, J. and Zhuang, X. (2011). Fast, three-dimensional super-resolution imaging of live cells. *Nat. Methods* **6**, 499-508. doi:10.1038/nmeth.1605
Keleman, K., Ribeiro, C. and Dickson, B. (2005). Comm function in commissural axon guidance: cell-autonomous sorting of Robo in vivo. *Nat. Neurosci.* **8**, 156-163. doi:10.1038/nn1388
Keller, P. and Stelzer, E. (2008). Quantitative in vivo imaging of entire embryos with digital scanned laser light sheet fluorescence microscopy. *Curr. Opin. Neurobiol.* **18**, 624-632. doi:10.1016/j.conb.2009.03.008

Kerkut, G., French, M. and Walker, R. (1970). The location of axonal pathways of identifiable neurones of Helix aspersa using the dye Procion yellow M-4R. *Comp. Biochem. Physiol.* **32**, 681-690. doi:10.1016/0010-406X(70)90820-0

Knobel, K. M., Jorgensen, E. M. and Bastiani, M. J. (1999). Growth cones stall and collapse during axon outgrowth in Caenorhabditis elegans. *Development* **126**, 4489-4498. doi:10.1242/dev.126.20.4489

Lakadamyali, M., Babcock, H., Bates, M., Zhuang, X. and Lichtman, J. (2012). 3D multicolor super-resolution imaging offers improved accuracy in neuron tracing. *PLoS ONE* **7**, e30826. doi:10.1371/journal.pone.0030826

Lemon, W. and Keller, P. (2015). Live imaging of nervous system development and function using light-sheet microscopy. *Mol. Reprod. Dev.* **82**, 605-618. doi:10.1002/mrd.22258

Leterrier, C., Dubey, P. and Roy, S. (2017). The nano-architecture of the axonal cytoskeleton. *Nat. Rev. Neurosci.* **18**, 713-726. doi:10.1038/nrn.2017.129

Letourneau, P. (2009). Actin in axons: stable scaffolds and dynamic filaments. *Results Probl. Cell Differ.* **48**, 65-90. doi:10.1007/400_2009_3

Li, H., Xu, F., Gao, S., Zhang, M., Xue, F., Xu, P. and Zhang, F. (2020). Live-SIMBA: an ImageJ plug-in for the universal and accelerated single molecule-guided Bayesian localization super resolution microscopy (SIMBA) method. *Biomed. Opt. Express* **11**, 5842-5859. doi:10.1364/BOE.404820

Liau, E., Yen, Y. and Chen, J. (2018). Visualization of motor axon navigation and quantification of axon arborization in mouse embryos using light sheet fluorescence microscopy. *J. Vis. Exp.* **135**, 57546. DOI:10.3791/57546

Lichtman, J., Livet, J. and Sanes, J. (2008). A technicolour approach to the connectome. *Nat. Rev. Neurosci.* **9**, 417-422. doi:10.1038/nrn2391

Liu, T., Upadhyayula, S., Milkie, D., Singh, V., Wang, K., Swinburne, I., Mosaliganti, K., Collins, Z., Hiscock, T., Shea, J. et al. (2018). Observing the cell in its native state: Imaging subcellular dynamics in multicellular organisms. *Science* **360**, eaaq1392. doi:10.1126/science.aaq1392

Livet, J., Weissman, T., Kang, H., Draft, R., Lu, J., Bennis, R., Sanes, J. and Lichtman, J. (2007). Transgenic strategies for combinatorial expression of fluorescent proteins in the nervous system. *Nature* **450**, 56-62. doi:10.1038/nature06293

Maglione, M. and Sigrist, S. (2013). Seeing the forest tree by tree: super-resolution light microscopy meets the neurosciences. *Nat. Neurosci.* **16**, 790-797. doi:10.1038/nn.3403

Mano, T., Albanese, A., Dodt, H., Erturk, A., Gradinaru, V., Treweek, J., Miyawaki, A., Chung, K. and Ueda, H. (2018). Whole-Brain Analysis of Cells and Circuits by Tissue Clearing and Light-Sheet Microscopy. *J. Neurosci.* **38**, 9330-9337. doi:10.1523/JNEUROSCI.1677-18.2018

McCormick, L. and Gupton, S. (2020). Mechanistic advances in axon pathfinding. *Curr. Opin. Cell Biol.* **63**, 11-19. doi:10.1016/j.ceb.2019.12.003

McElmurry, K., Stone, J., Ma, D., Lamoureux, P., Zhang, Y., Steidemann, M., Fix, L., Huang, F., Miller, K. and Suter, D. (2020). Dynein-mediated microtubule translocation powering neurite outgrowth in chick and Aplysia neurons requires microtubule assembly. *J. Cell Sci.* **133**, jcs232983. doi:10.1242/jcs.232983

McLaughlin, T. and O'Leary, D. (2005). Molecular gradients and development of retinotopic maps. *Annu. Rev. Neurosci.* **28**, 327-355. doi:10.1146/annurev.neuro.28.061604.135714

Meka, D., Scharrenberg, R., Zhao, B., Kobler, O., König, T., Schaefer, I., Schwanke, B., Klykov, S., Richter, M., Eggert, D. et al. (2019). Radial somatic F-actin organization affects growth cone dynamics during early neuronal development. *EMBO Rep.* **20**, e47743. doi:10.15252/embr.201947743

Mortal, S., Iseppon, F., Perissinotto, A., D'Este, E., Cojoc, D., Napolitano, L. and Torre, V. (2017). Actin waves do not boost neurite outgrowth in the early stages of neuron maturation. *Front. Cell Neurosci.* **11**, 402. doi:10.3389/fncel.2017.00402

Moyle, M., Barnes, K., Kuchroo, M., Gonopolskiy, A., Duncan, L., Sengupta, T., Shao, L., Guo, M., Santella, A., Christensen, R. et al. (2021). Structural and developmental principles of neuropil assembly in C. elegans. *Nature* **591**, 99-104. doi:10.1038/s41586-020-03169-5

Mulder, J., Aguado, T., Keimpema, E., Barabás, K., Ballester Rosado, C., Nguyen, L., Monory, K., Marsicano, G., Di Marzo, V., Hurd, Y. et al. (2008). Endocannabinoid signaling controls pyramidal cell specification and long-range axon patterning. *Proc. Natl. Acad. Sci. USA* **105**, 8760-8765. doi:10.1073/pnas.0803545105

Murray, M. J., Merritt, D. J., Brand, A. H. and Whitington, P. M. (1998). In vivo dynamics of axon pathfinding in the Drosophila CNS: a time- lapse study of an identified motorneuron. *J. Neurobiol.* **37**, 607-621. doi:10.1002/(SICI)1097-4695(199812)37:4<607::AID-NEU9>3.0.CO;2-Q

Nair, D., Hosy, E., Petersen, J., Constals, A., Giannone, G., Choquet, D. and Sibarita, J. (2013). Super-resolution imaging reveals that AMPA receptors inside synapses are dynamically organized in nanodomains regulated by PSD95. *J. Neurosci.* **33**, 13204-13224. doi:10.1523/JNEUROSCI.2381-12.2013

Nakamoto, M., Cheng, H. J., Friedman, G. C., McLaughlin, T., Hansen, M. J., Yoon, C. H., O'Leary, D. D. and Flanagan, J. G. (1996). Topographically specific effects of ELF-1 on retinal axon guidance in vitro and retinal axon mapping in vivo. *Cell* **86**, 755-766. doi:10.1016/S0092-8674(00)80150-6

Nichols, E. and Smith, C. (2019a). Synaptic-like vesicles facilitate pioneer axon invasion. *Curr. Biol.* **29**, 2652-2664.e4. doi:10.1016/j.cub.2019.06.078

Nichols, E. and Smith, C. (2019b). Pioneer axons employ Cajal's battering ram to enter the spinal cord. *Nat. Commun.* **10**, 562. doi:10.1038/s41467-019-08421-9

Norris, A. D., Dyer, J. O. and Lundquist, E. A. (2009). The Arp2/3 complex, UNC-115/abLIM, and UNC-34/Enabled regulate axon guidance and growth cone filopodia formation in Caenorhabditis elegans. *Neural Dev.* **4**, 38. doi:10.1186/1749-8104-4-38

Nozumi, M., Nakatsu, F., Katoh, K. and Igarashi, M. (2017). Coordinated movement of vesicles and actin bundles during nerve growth revealed by superresolution microscopy. *Cell Rep* **18**, 2203-2216. doi:10.1016/j.celrep.2017.02.008

Nägerl, U., Willig, K., Hein, B., Hell, S. and Bonhoeffer, T. (2008). Live-cell imaging of dendritic spines by STED microscopy. *Proc. Natl. Acad. Sci. USA* **105**, 18982-18987. doi:10.1073/pnas.0810028105

O'Donnell, M., Chance, R. and Bashaw, G. (2009). Axon growth and guidance: receptor regulation and signal transduction. *Annu. Rev. Neurosci.* **32**, 383-412. doi:10.1146/annurev.neuro.051508.135614

Pan, Y., Livet, J., Sanes, J., Lichtman, J. and Schier, A. (2011). Multicolor Brainbow imaging in zebrafish. *Cold Spring Harb. Protoc.* **2011**, pdb.prot5546. doi:10.1101/pdb.prot5546

Pan, C., Cai, R., Quacquarelli, F., Ghasemigharagoz, A., Lourbopoulos, A., Matryba, P., Plesnila, N., Dichgans, M., Hellal, F. and Ertürk, A. (2016). Shrinkage-mediated imaging of entire organs and organisms using uDISCO. *Nat. Methods* **13**, 859-867. doi:10.1038/nmeth.3964

Pignata, A., Ducuing, H., Boubakar, L., Gardette, T., Kindbeiter, K., Bozon, M., Tauszig-Delamasure, S., Falk, J., Thoumine, O. and Castellani, V. (2019). A spatiotemporal sequence of sensitization to slits and semaphorins orchestrates commissural axon navigation. *Cell Rep.* **29**, 347-362. doi:10.1016/j.celrep.2019.08.098

Poulain, F. and Sobel, A. (2010). The microtubule network and neuronal morphogenesis: dynamic and coordinated orchestration through multiple players. *Mol. Cell. Neurosci.* **43**, 15-32. doi:10.1016/j.mcn.2009.07.012

Poulain, F. E. and Chien, C. B. (2013). Proteoglycan-mediated axon degeneration corrects pretarget topographic sorting errors. *Neuron* **78**, 49-56. doi:10.1016/j.neuron.2013.02.005

Quinn, C. C., Pfeil, D. S. and Wadsworth, W. G. (2008). CED-10/Rac1 mediates axon guidance by regulating the asymmetric distribution of MIG-10/lamellipodin. *Curr. Biol.* **18**, 808-813. doi:10.1016/j.cub.2008.04.050

Ramón y Cajal, S. (1991). New ideas on the structure of the nervous system in man and vertebrates. *J. Cogn. Neurosci.* **3**, 300-301. doi:10.1162/jocn.1991.3.3.300

Renier, N., Wu, Z., Simon, D., Yang, J., Ariel, P. and Tessier-Lavigne, M. (2014). iDISCO: a simple, rapid method to immunolabel large tissue samples for volume imaging. *Cell* **159**, 896-910. doi:10.1016/j.cell.2014.10.010

Robles, E., Filosa, A. and Baier, H. (2013). Precise lamination of retinal axons generates multiple parallel input pathways in the tectum. *J. Neurosci.* **33**, 5027-5039. doi:10.1523/JNEUROSCI.4990-12.2013

Roy, S., Coffee, P., Smith, G., Liem, R., Brady, S. and Black, M. (2000). Neurofilaments are transported rapidly but intermittently in axons: implications for slow axonal transport. *J. Neurosci.* **20**, 5027-5039. doi:10.1523/JNEUROSCI.20-18-06849.2000

Ruthel, G. and Banker, G. (1998). Actin-dependent anterograde movement of growth-cone-like structures along growing hippocampal axons: a novel form of axonal transport? *Cell Motil. Cytoskeleton* **40**, 160-173. doi:10.1002/(SICI)1097-0169(1998)40:2<160::AID-CM5>3.0.CO;2-J

Saez, T., Fernandez Bessone, I., Rodriguez, M., Alloatti, M., Otero, M., Cromberg, L., Pozo Devoto, V., Oubiña, G., Sosa, L., Buffone, M. et al. (2020). Kinesin-1-mediated axonal transport of CB1 receptors is required for cannabinoid-dependent axonal growth and guidance. *Development* **147**, dev184069. doi:10.1242/dev.184069

Santiago-Medina, M., Gregus, K., Nichol, R., O'Toole, S. and Gomez, T. (2015). Regulation of ECM degradation and axon guidance by growth cone invadosomes. *Development* **142**, 486-496. doi:10.1242/dev.108266

Santos, T. E., Schaffran, B., Broguière, N., Meyn, L., Zenobi-Wong, M. and Bradke, F. (2020). Axon growth of CNS neurons in three dimensions is amoeboid and independent of adhesions. *Cell Rep.* **32**, 107907. doi:10.1016/j.celrep.2020.107907

Schaefer, A. W., Kabir, N. and Forscher, P. (2002). Filopodia and actin arcs guide the assembly and transport of two populations of microtubules with unique dynamic parameters in neuronal growth cones. *J. Cell Biol.* **158**, 139-152. doi:10.1083/jcb.200203038

Sharonov, A. and Hochstrasser, R. (2006). Wide-field subdiffraction imaging by accumulated binding of diffusing probes. *Proc. Natl. Acad. Sci. USA* **103**, 18911-18916. doi:10.1073/pnas.0609643104

Shcherbakova, D., Sengupta, P., Lippincott-Schwartz, J. and Verkhusha, V. (2014). Photocontrollable fluorescent proteins for superresolution imaging. *Annu. Rev. Biophys.* **43**, 303-329. doi:10.1146/annurev-biophys-051013-022836

Siddig, S., Aufmkolk, S., Doose, S., Jobin, M., Werner, C., Sauer, M. and Calebiro, D. (2020). Super-resolution imaging reveals the nanoscale organization of metabotropic glutamate receptors at presynaptic active zones. *Sci. Adv.* **6**, eaay7193. doi:10.1126/sciadv.aay7193

Slater, P., Cammarata, G., Samuelson, A., Magee, A., Hu, Y. and Lowery, L. (2019). XMAP215 promotes microtubule-F-actin interactions to regulate growth cone microtubules during axon guidance in Xenopus laevis. *J. Cell Sci.* **132**, jcs224311. doi:10.1242/jcs.224311

Sotelo, C. (2002). The chemotactic hypothesis of Cajal: a century behind. *Prog. Brain Res.* **136**, 11-20. doi:10.1016/S0079-6123(02)36004-7

Spead, O. and Poulain, F. (2020). Trans-axonal signaling in neural circuit wiring. *Int. J. Mol. Sci.* **21**, 5170. doi:10.3390/ijms21145170

Stoeckli, E. (2018). Understanding axon guidance: are we nearly there yet? *Development* **145**, dev151415. doi:10.1242/dev.151415

Stretton, A. and Kravitz, E. (1968). Neuronal geometry: determination with a technique of intracellular dye injection. *Science* **162**, 132-134. doi:10.1126/science.162.3849.132

Suárez, R., Gobius, I. and Richards, L. (2014). Evolution and development of interhemispheric connections in the vertebrate forebrain. *Front. Hum. Neurosci.* **8**, 497. doi:10.3389/fnhum.2014.00497

Szalai, A., Siarry, B., Lukin, J., Giusti, S., Unsain, N., Cáceres, A., Steiner, F., Tinnefeld, P., Refojo, D., Jovin, T. et al. (2021). Super-resolution imaging of energy transfer by intensity-based STED-FRET. *Nano Lett.* **21**, 2296-2303. doi:10.1021/acs.nanolett.1c00158

Tessier-Lavigne, M. and Goodman, C. (1996). The molecular biology of axon guidance. *Science* **274**, 1123-1133. doi:10.1126/science.274.5290.1123

Tojima, T., Itofusa, R. and Kamiguchi, H. (2014). Steering neuronal growth cones by shifting the imbalance between exocytosis and endocytosis. *J. Neurosci.* **34**, 7165-7178. doi:10.1523/jneurosci.5261-13.2014

Tomer, R., Khairy, K., Amat, F. and Keller, P. (2012). Quantitative high-speed imaging of entire developing embryos with simultaneous multiview light-sheet microscopy. *Nat. Methods* **9**, 755-763. doi:10.1038/nmeth.2062

Trotter, J., Hao, J., Maxeiner, S., Tsetsenis, T., Liu, Z., Zhuang, X. and Südhof, T. (2019). Synaptic neurexin-1 assembles into dynamically regulated active zone nanoclusters. *J. Cell Biol.* **218**, 2677-2698. doi:10.1083/jcb.201812076

Ueda, H., Ertürk, A., Chung, K., Gradinaru, V., Chédotal, A., Tomancak, P. and Keller, P. (2020). Tissue clearing and its applications in neuroscience. *Nat. Rev. Neurosci.* **21**, 61-79. doi:10.1038/s41583-019-0250-1

van der Kooy, D. and Steinbusch, H. (1980). Simultaneous fluorescent retrograde axonal tracing and immunofluorescent characterization of neurons. *J. Neurosci. Res.* **5**, 479-484. doi:10.1002/jnr.490050603

van Krugten, J., Taris, K. and Peterman, E. (2021). Imaging adult C. elegans live using light-sheet microscopy. *J. Microsc.* **281**, 214-223. doi:10.1111/jmi.12964

Vassilopoulos, S., Gibaud, S., Jimenez, A., Caillol, G. and Leterrier, C. (2019). Ultrastructure of the axonal periodic scaffold reveals a braid-like organization of actin rings. *Nat. Commun.* **10**, 5803. doi:10.1038/s41467-019-13835-6

Vigouroux, R., Cesar, Q., Chédotal, A. and Nguyen-Ba-Charvet, K. (2020). Revisiting the role of Dcc in visual system development with a novel eye clearing method. *eLife* **9**, e51275. doi:10.7554/eLife.51275

Voie, A., Burns, D. and Spelman, F. (1993). Orthogonal-plane fluorescence optical sectioning: three-dimensional imaging of macroscopic biological specimens. *J. Microsc.* **170**, 229-236. doi:10.1111/j.1365-2818.1993.tb03346.x

Wan, Y., McDole, K. and Keller, P. (2019). Light-sheet microscopy and its potential for understanding developmental processes. *Annu. Rev. Cell Dev. Biol.* **35**, 655-681. doi:10.1146/annurev-cellbio-100818-125311

Wang, L. and Brown, A. (2002). Rapid movement of microtubules in axons. *Curr. Biol.* **12**, 1496-1501. doi:10.1016/S0960-9822(02)01078-3

Wang, L. and Marquardt, T. (2013). What axons tell each other: axon-axon signaling in nerve and circuit assembly. *Curr. Opin. Neurobiol.* **23**, 974-982. doi:10.1016/j.conb.2013.08.004

Wang, L., Ho, C., Sun, D., Liem, R. and Brown, A. (2000). Rapid movement of axonal neurofilaments interrupted by prolonged pauses. *Nat. Cell Biol.* **2**, 137-141. doi:10.1038/35004008

Wang, T., Li, W., Martin, S., Papadopulos, A., Joensuu, M., Liu, C., Jiang, A., Shamsollahi, G., Amor, R., Lanoue, V. et al. (2020). Radial contractility of actomyosin rings facilitates axonal trafficking and structural stability. *J. Cell Biol.* **219**, e201902001. doi:10.1083/jcb.201902001

Weissman, T. and Pan, Y. (2015). Brainbow: new resources and emerging biological applications for multicolor genetic labeling and analysis. *Genetics* **199**, 293-306. doi:10.1534/genetics.114.172510

White, J., Southgate, E., Thomson, J. and Brenner, S. (1986). The structure of the nervous system of the nematode Caenorhabditis elegans. *Philos. Trans. R. Soc. Lond. B Biol. Sci.* **314**, 1-340. doi:10.1098/rstb.1986.0056

Willard, M., Wiseman, M., Levine, J. and Skene, P. (1979). Axonal transport of actin in rabbit retinal ganglion cells. *J. Cell Biol.* **81**, 581-591. doi:10.1083/jcb.81.3.581

Wu, Y., Ghitani, A., Christensen, R., Santella, A., Du, Z., Rondeau, G., Bao, Z., Colón-Ramos, D. and Shroff, H. (2011). Inverted selective plane illumination microscopy (iSPIM) enables coupled cell identity lineaging and neurodevelopmental imaging in Caenorhabditis elegans. *Proc. Natl. Acad. Sci. USA* **108**, 17708-17713. doi:10.1073/pnas.1108494108

Wuerker, R. and Kirkpatrick, J. (1972). Neuronal microtubules, neurofilaments, and microfilaments. *Int. Rev. Cytol.* **33**, 45-75. doi:10.1016/S0074-7696(08)61448-5

Xu, K., Zhong, G. and Zhuang, X. (2013). Actin, spectrin, and associated proteins form a periodic cytoskeletal structure in axons. *Science* **339**, 452-456. doi:10.1126/science.1232251

Xu, F., Zhang, M., He, W., Han, R., Xue, F., Liu, Z., Zhang, F., Lippincott-Schwartz, J. and Xu, P. (2017). Live cell single molecule-guided Bayesian localization super resolution microscopy. *Cell Res.* **27**, 713-716. doi:10.1038/cr.2016.160

Zallen, J. A., Yi, B. A. and Bargmann, C. I. (1999). The conserved immunoglobulin superfamily member SAX-3/Robo directs multiple aspects of axon guidance in C. *elegans*. *Cell* **92**, 217-227. doi:10.1016/S0092-8674(00)80916-2

Zang, Y., Chaudhari, K. and Bashaw, G. (2021). New insights into the molecular mechanisms of axon guidance receptor regulation and signaling. *Curr. Top. Dev. Biol.* **142**, 147-196. doi:10.1016/bs.ctdb.2020.11.008

Zecca, A., Dyballa, S., Voltes, A., Bradley, R. and Pujades, C. (2015). The order and place of neuronal differentiation establish the topography of sensory projections and the entry points within the hindbrain. *J. Neurosci.* **35**, 7475-7486. doi:10.1523/JNEUROSCI.3743-14.2015

Zhang, Y., Nichols, E., Zellmer, A., Guldner, I., Kankel, C., Zhang, S., Howard, S. and Smith, C. (2019). Generating intravital super-resolution movies with conventional microscopy reveals actin dynamics that construct pioneer axons. *Development* **146**, dev171512. doi:10.1242/dev.171512

Zheng, Z., Lauritzen, J., Perlman, E., Robinson, C., Nichols, M., Milkie, D., Torrens, O., Price, J., Fisher, C., Sharifi, N. et al. (2018). A Complete Electron Microscopy Volume of the Brain of Adult Drosophila melanogaster. *Cell* **174**, 730-743. doi:10.1016/j.cell.2018.06.019

Zhou, R., Han, B., Xia, C. and Zhuang, X. (2019). Membrane-associated periodic skeleton is a signaling platform for RTK transactivation in neurons. *Science* **365**, 929-934. doi:10.1126/science.aaw5937

Zou, Y., Stoeckli, E., Chen, H. and Tessier-Lavigne, M. (2000). Squeezing axons out of the gray matter: a role for slit and semaphorin proteins from midline and ventral spinal cord. *Cell* **102**, 363-375. doi:10.1016/S0092-8674(00)00041-6